Earth and Planetary Science Letters 511 (2019) 55–66

Contents lists available at ScienceDirect

Earth and Planetary Science Letters

www.elsevier.com/locate/epsl

The evolution of the Levantine Iron Age geomagnetic Anomaly captured in Mediterranean sediments

Annemarieke Béguin [a,*], Amalia Filippidi [b], Gert J. de Lange [b], Lennart V. de Groot [a]

[a] Paleomagnetic Laboratory Fort Hoofddijk, Department of Earth Sciences, Faculty of Geosciences, Utrecht University, Utrecht, the Netherlands
[b] Department of Earth Sciences-Geochemistry, Faculty of Geosciences, Utrecht University, Utrecht, the Netherlands

ARTICLE INFO

Article history:
Received 6 February 2018
Received in revised form 13 November 2018
Accepted 10 January 2019
Available online 4 February 2019
Editor: B. Buffett

Keywords:
geomagnetic field
paleointensity
Levant geomagnetic high

ABSTRACT

The geomagnetic field can vary dramatically over only decades and thousands of kilometers; the Levantine Iron Age geomagnetic Anomaly (LIAA) is probably the best-known example of such short-lived feature of the Earth's magnetic field. Yet, the size, shape and temporal variations of this phenomenon are currently still enigmatic. Here we provide continuous full-vector records of the variations in the geomagnetic field from three marine sediment cores from the Mediterranean, to better constrain the LIAA in time and space. The cores are located (1) between Spain and Morocco (Alboran), (2) East of Calabria, Italy (Taranto Gulf), and (3) North of the Nile Delta (Levant). Geomagnetic field variations between 6000 BC and 1000 AD are captured for a total of 681 samples. Rock magnetic analyses indicate the sediment cores as reliable recorders for geomagnetic field variations. Between 750 and 250 BC, high intensities are observed for the Levant and Taranto Gulf core, with their peak – 150 ZAm^2 at 500 BC – shortly after the occurrence of the LIAA. Low paleointensities are obtained from the Alboran core providing a western limit of the extent of the LIAA until at least 250 BC. From 500 BC onwards the location of the highest paleointensities moves slightly westwards while diminishing in intensity. The LIAA moves from 40 to 55° East at 1000 BC to ~25° East at 0 AD, while decaying from ~150 ZAm^2 to ~110 ZAm^2 in the same time span. This results in a westward movement of 15–30° in 1000 yr.

1. Introduction

Beyond its long-term-average dipolar behavior, the geomagnetic field can vary dramatically in direction and intensity over just decades and only thousands of kilometers. The most prominent example of such behavior is arguably the 'Levantine Iron Age Geomagnetic Anomaly' (LIAA), a period of non-geocentral axial dipolar (GAD) magnetic directions and high geomagnetic field strengths (virtual axial dipole moment (VADM) > 140 ZAm^2) reported for the Levant between ~1000 and ~750 BC (e.g. Ben-Yosef et al., 2017, 2009; Shaar et al., 2011, 2017, 2016). Within the LIAA two peaks in the geomagnetic field strength (spikes of VADM > 160 ZAm^2) were recently identified at 980 and 740 BC (Shaar et al., 2016). The size, shape and temporal evolution of the LIAA, however, still are largely enigmatic. Recently, Shaar et al. (2017) characterized the spatial and temporal extent of the LIAA eastwards of the Levant. Understanding rapid and short-lived fluctuations in intensity, such as LIAA, is crucial to temporally and spatially constrain variations in the Earth's magnetic field, which in turn improves our understanding of the behavior of the Earth's outer core, as this is where the geomagnetic field is generated.

The Levant region boasts a wealth of well-dated archeomagnetic artifacts, which are ideal recorders of the intensity of the Earth's magnetic field. These artifacts take spot-readings of the geomagnetic field as they cool, and can therefore provide a high-fidelity record of geomagnetic variations for this region – provided that they are accurately dated. Over the past decade, many studies have contributed to a relatively coherent intensity record for this region, resulting in the 'Levant Archeomagnetic Compilation' (LAC) (Shaar et al., 2016). As most of these recorders are not in-situ (e.g. ceramic sherds), it is impossible to obtain reliable paleodirections from them. Hence, the directional records are not continuous throughout time and the variations in geomagnetic declination and inclination are less well constrained for this region compared to the amount of available paleointensity data.

Recent research on the Canary Islands – approximately 60 degrees to the West of the Levant region – reveals high paleointensities (i.e. VADMs ~ 120 ZAm^2); this peak, however, is poorly constrained in time. It may be coeval with the LIAA, but also up to 500 yr younger (de Groot et al., 2015; Kissel et al., 2015). A coeval occurrence in the Levant and the Canary Islands would im-

* Corresponding author.
E-mail address: a.beguin@uu.nl (A. Béguin).

https://doi.org/10.1016/j.epsl.2019.01.021
0012-821X/

Fig. 1. Mediterranean Sea with core locations. The cores are located (1) between Spain and Morocco (Alboran – blue star), (2) East of Calabria, Italy (Taranto Gulf – red star), and (3) North of the Nile Delta (Levant – orange star). (For interpretation of the colors in the figure(s), the reader is referred to the web version of this article.)

Table 1
Three marine sediment cores taken from the Mediterranean Sea, giving the name, region, location and number of samples taken from each core section.

Piston core	Area	Latitude	Longitude	Water depth	Section	Length (cm)	Number of samples
MT16	Alboran	36°01.5′N	3°51.88′W	1257 m	#9	35	54
					#8	100	158
MP49	Taranto Gulf	39°50.07′N	17°48.06′E	267 m	#9	100	157
					#8	100	158
PS009	Levant	32°07.7′N	34°24.4′E	522 m	#6	100	154

ply a rather large spatial extent of the LIAA; if the peaks in the Levant and the Canary Islands differ by as much as 500 years, a westward movement could explain the observations, although the behavior of regional peaks in the intensity of the geomagnetic field are often more complex (de Groot et al., 2013). Hervé et al. (2017) recently presented high intensities for Western Europe between 1000 and 600–500 BC, and constrain the LIAA to the Northwest.

To better constrain the behavior of the LIAA in time and space, and assess its potential westward movement, continuous full-vector records (declination, inclination, and relative intensity) are needed for the region of interest, which extends from the Levant westward to the Canary Islands, and potentially even the Azores (Di Chiara et al., 2014), and Texas, USA (Bourne et al., 2016). Here, we present three new, continuous, (relative) full-vector records from marine sediment cores taken in the Mediterranean Sea, located (1) off the Israeli coast ∼80 km SSW of Haifa, (2) in the Taranto Gulf ∼27 km SSW of Gallipoli (Italy), and (3) in the West Alboran Sea ∼85 km SSE of Malaga, Spain (Fig. 1, Table 1). For each of the three cores, an age-depth model is available or produced; the sedimentation rate in the analyzed cores is high, typically 20 to 65 cm/kyr, resulting in 15–50 yr per paleomagnetic sample of 1 cm^3. In spite of these high sedimentation rates geomagnetic fluctuations shorter than 15–50 yr – such as the two geomagnetic spikes reported within the LIAA (Shaar et al., 2017) – will go undetected, but the somewhat longer trends of the LIAA on decadal to centennial timescales are captured continuously and in great detail.

Sample material permitting, the parts that recorded the period centered around the LIAA were sampled in all three cores. The longest span sampled is ∼6000 BC to 1000 AD for the Alboran core. The sediment cores underwent an independent assessment of the reliability of the cores as recorders of geomagnetic field variations by high- and low-field experiments, and thermal rock magnetic analyses. If these proxies are constant throughout the cores, the reliability and credibility of both the paleodirections and paleointensities is greatly enhanced. After these preliminary analyses, 681 samples in total underwent alternating field demagnetization to obtain the direction of the stored geomagnetic field; (relative) declination and inclination, followed by a pseudo-Thellier intensity experiment (Tauxe et al., 1995) to obtain the relative intensity through the sediment cores. The relative declination and intensity records are then converted to absolute declinations and intensities using literature data from the GEOMAGIA database (Brown et al., 2015), to produce absolute, full-vector records of variations in the Earth's magnetic field.

2. Geological setting and sampling

The three cores (PS009, MP49, and MT16) were taken on different cruises (Table 1). The MT16 piston core was taken during the RV Tyro cruise in 1993. Piston core MP49 was recovered during the RV Pelagia cruise 'MACCHIATO' in 2009, and is located at the same site as sediment core DP30 (39.835°N 17.801°E) (Goudeau et al., 2015). The Levantine piston core, PS009, was taken during the PASSAP cruise with RV Pelagia to the eastern Mediterranean (Hennekam and de Lange, 2012; Hennekam et al., 2014). This area is known to be largely influenced by sedimentation from the Nile (Almogi-Labin et al., 2009; Venkatarathnam and Ryan, 1971).

Paleomagnetic samples were taken from the sections of interest – i.e. at least containing the interval before, during and after the LIAA (∼2000 BC-0 AD). From the Alboran (MT16), Taranto Gulf (MP49) and Levant (PS009) cores, 212, 315 and 154 samples were taken, respectively. Two rows of plastic cubic sample cups with an inner volume of 1 cm^3 were pushed into the sediment such that the cups in each row touched each other, ensuring a continuous sampling, resulting in approximately 150 samples per meter sediment, i.e. 150 samples per 100 cm core. The two rows were offset by half a cube to increase the resolution (Fig. 2). For rock-magnetic analyses extra samples were taken approximately every 20 cm, resulting in 4–5 samples per meter sediment. The samples for rock magnetic analyses were dried in an oven at 50 °C to remove excess water. To detect the occurrence of sulphide-oxides that are known to adversely interfere with alternating field demagnetizations and to potentially discriminate between a biogenic and

Fig. 2. Sampling of the cores. Two rows of 1 cm^3 cubes are pushed into the sediment; the two rows are offset by half a cube to increase the sampling resolution. Yellowish colors on some cubes is light reflection. The sample cubes were numbered row by row from top to bottom of the core. To reduce oxidation of the sediment, the small holes in the plastic cubes were sealed with acid-free silicone paste and the samples were stored in the fridge.

diagenetic origin, another three samples were taken from each core for FORC-measurements (mass between 13 and 55 mg); the FORCs where completed within hours after taking a sample out of the refrigerator.

The age models are based on combinations of ^{14}C and ^{210}Pb measurements. For the Alboran (MT16) core the age of the samples ranges between ∼2000–8000 cal yr BP, for the Taranto Gulf (MP49) core the measured samples range between ∼1000–4000 cal yr BP, and the Levant (PS009) samples cover ∼1000–5000 cal yr BP.

3. Geo-chronology

The ^{210}Pb measurements were done on freeze–dried and grounded sediments, whereas the radiocarbon ^{14}C ages were performed on clean, hand-picked mixed planktonic foraminifera (size faction >63 µm). The analyses were performed for ^{210}Pb at ENEA – Marine Environmental Research Center, Italy, and for ^{14}C using accelerator mass spectrometry (AMS) at Poznan Radiocarbon Laboratory, Poland.

Conventional ^{14}C ages were calibrated using the program CALIB 6.0 (Marine 09) (Stuiver and Reimer, 1993; Stuiver et al., 1998) with a regional reservoir age correction (ΔR) for Taranto Gulf core of 121 ± 60 yr and for W. Mediterranean 148 ± 35 yr (Table 2). ^{210}Pb measurements showed that for MP49PC there is a good recovery of the topmost sediments with little mixing processes, whereas the most recent sediments have not been recovered for MT16. The ^{14}C measurements showed a nearly linear relation between the age of the sediments and depth in both the Alboran and Taranto Gulf cores (Fig. 3a & Fig. 3b). For the Levant core (Fig. 3c), age model details are given in Hennekam et al. (2014).

The sedimentation rates of the Alboran and Taranto Gulf cores are constant at ∼21 and ∼71 cm/kyr, respectively. The sedimentation rate of the Levant core changes with depth from ∼19 at the bottom, to ∼37 cm/kyr for the top part of this core.

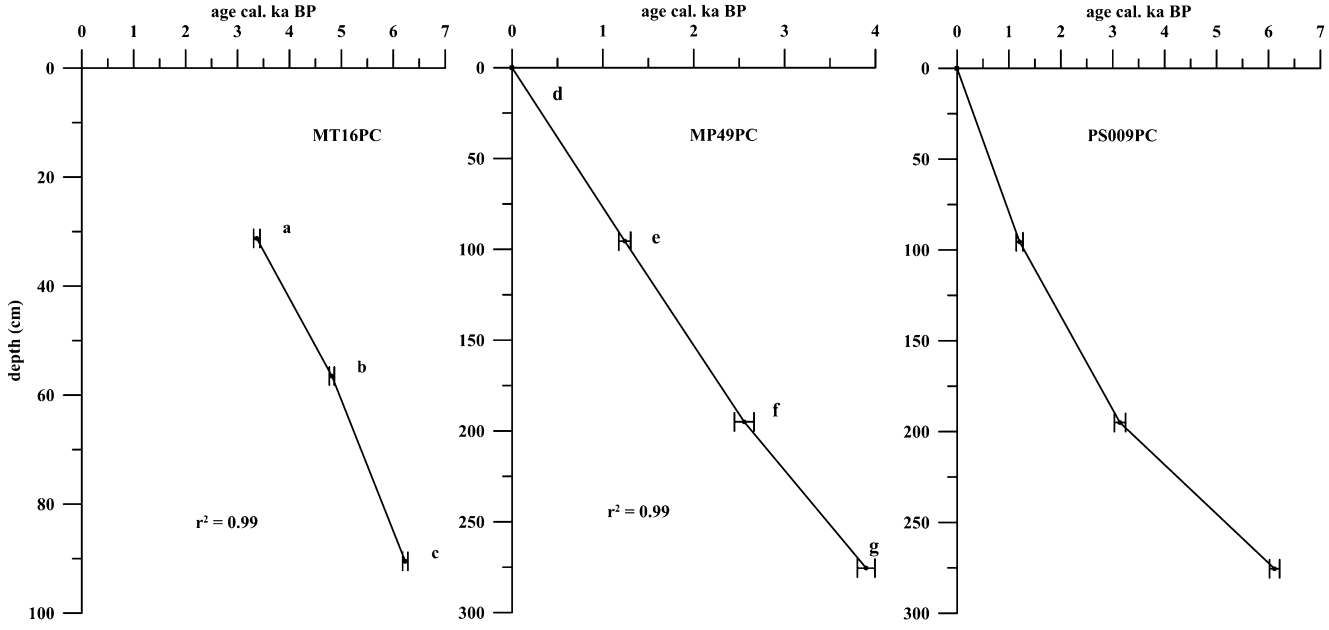

Fig. 3. Age models for the Alboran (MT16), Taranto Gulf (MP49) and Levant (PS009) cores. Depth within the core to calibrated ages BP, details of the dating points per core are in Table 2.

Table 2
Core chronology – ^{14}C ages, reservoir age corrections and calibrated ages for cores MT16 and MP49PC; Reservoir age corrections for all dating point used, is ∼400 yr (included in calibration program Marine 09); additional regional reservoir age correction for Adriatic Sea (MP49PC) $\Delta R = 121 \pm 60$ (Hughen et al., 2004), and for W. Mediterranean core (MT16) $\Delta R = 148 \pm 35$ yr (Siani et al., 2000).

	Lab code	Sample	Av. depth (cm)	^{14}C age (BP) $\pm 1\sigma$ error (yr)	ΔR (yr)	1σ age cal BP
a	*Poz-74760*	*MT16#9 31–32 cm*	*31,25*	*3625 ± 30 BP*	*148 ± 35 BP*	*3370 ± 60*
b	*Poz-74671*	*MT16#8 21–22 cm*	*56,5*	*4740 ± 30 BP*	*148 ± 35 BP*	*4817 ± 48*
c	*Poz-74672*	*MT16PC#8 55–56 cm*	*90,5*	*5960 ± 40 BP*	*148 ± 35 BP*	*6231 ± 50*
e	*Poz-74673*	*MP49PC#9 9.5–11.5 cm*	*95,5*	*1815 ± 30 BP*	*121 ± 60 BP*	*1241 ± 65*
f	*Poz-74674*	*MP49PC#8 9–11 cm*	*195*	*2915 ± 35 BP*	*121 ± 60 BP*	*2556 ± 108*
g	*Poz-74675*	*MP49PC#8 89.5–91.5 cm*	*275,5*	*4035 ± 30 BP*	*121 ± 60 BP*	*3898 ± 97*

4. Methods

4.1. Rock-magnetic analyses

To assess the reliability of the marine sediment cores as recorders of geomagnetic field variations, three different rock-magnetic proxies were studied. Firstly, the magnetic carriers and minerals within the cores were characterized by analyzing samples on the Curie Balance (Mullender et al., 1993). The magnetization of a sample was measured while heating them in seven cycles; the peak temperatures were set to 150, 250, 350, 400, 450, 500 and 700 °C. After reaching a peak temperature, the temperature was lowered by 100 °C to check for permanent alteration of the signal. Curie temperatures for samples are derived by the two-tangent method.

Secondly, the domain state of the magnetic carriers from the clay cores was assessed by determining high-field magnetic properties (saturation magnetization (Ms), remanent saturation magnetization (Mr), coercive force (Hc), and remanent coercive force (Hcr)) derived from hysteresis loops and back field (or DCD) curves, samples were analyzed using a MicroSense vibrating sample magnetometer (VSM). The Mr/Ms and Hcr/Hc ratios were expressed in a Day plot (Day et al., 1977; Dunlop, 2002). Consistent domain states throughout the cores further establish the cores as reliable recorders of variations in both paleomagnetic directions and intensities through time. To characterize the potential occurrence and origin of sulphide-oxides first order reversal curves (FORCs) were measured on a Princeton alternating gradient force magnetometer, PMC Model 2900. As especially diagenetic greigite is known to produce adverse gyro-remanent magnetizations (GRMs) when demagnetized using alternating fields, it is important to determine the origin of the greigite. To discriminate between diagenetic greigite and biogenic greigite – which is formed during sediment accumulation, hence carries a primary magnetization – FORCs were measured (Vasiliev et al., 2008) and interpreted with FORCinel (Harrison and Feinberg, 2008). Central ridges within the FORC diagrams indicate biogenic greigite.

Lastly, mass-normalized magnetic susceptibility of all samples was measured at room temperature using an AGICO MFK1 susceptometer, indicating the response of the samples to a small applied (alternating) magnetic field. Large and abrupt differences in the susceptibility in the core indicate variations in magnetic composition and concentration of magnetic material, which may hamper the magnetic intensity proxy in particular. A gradual increase of the susceptibility with depth implies an increasing concentration of magnetic material. This may be a sign of the removal of water from the sediment, and hence indicate compaction; the water content was also measured directly by comparing the weight between fresh and completely dried material. The magnetic susceptibility together with the susceptibility of the ARM is used to calculate the grainsize sensitive kARM/k ratio (Banerjee et al., 1981; King et al., 1982; Liu et al., 2012). As the sedimentary regime is believed to be relatively constant, homogeneous results are expected from the same core.

4.2. Paleomagnetic directions

The Natural Remanent Magnetization (NRM) of the samples was measured with a robotized 2G DC-SQUID cryogenic magnetometer (Mullender et al., 2016). The NRM of the samples were demagnetized using alternating magnetic fields. The AF fields increased in 14 steps: 5, 10, 15, 20, 25, 30, 35, 40, 50, 60, 70, 80, 90, 100 mT, after each demagnetization step the remaining magnetization was measured. Declination and inclination values were obtained from the forthcoming Zijderveld diagrams using paleomagnetism.org (Koymans et al., 2016). Since the marine sediment cores are not orientated, the obtained declination records are relative records of changes in the declination, the average declination is set to 0°. Samples with a Mean Angular Deviation (MAD) greater than 10° are removed from the records. Also, if an overprint on the NRM is not removed with AF fields < 30 mT the samples are not suitable for paleointensity analyses since the NRM segment left is too small to be reliably interpreted, therefore these samples are removed from the records and the interpreted directions are rejected.

4.3. Relative paleointensity analyses

The relative paleointensity of the core samples were measured using the pseudo-Thellier protocol (Tauxe et al., 1995). After the NRM of the samples was fully demagnetized, a series of anhysteretic remanent magnetizations (ARMs) was imparted on the sediment using the same 14 alternating field steps (5–100 mT) using a DC field of 40 μT. After each field step the acquired magnetization was measured. To check whether the same grains that carried the NRM acquired the ARMs, the ARMs of the samples were stepwise demagnetized using the same 14 alternating fields again, while measuring in between the field steps.

The ARM gained was plotted versus NRM remaining resulting in an Arai plot. The section for which the same grains carry the magnetization, i.e. the part for which the NRM demagnetization versus the ARM demagnetization yielded a linear relation (typically 20–60 mT), was selected and the slope of the Arai plot was determined. This slope is the pseudo-Thellier value and is a proxy for the relative paleointensity for all measured samples from the same core.

The R^2-value is determined for the resulting Arai plots, samples with R^2-values < 0.980 are not considered for further interpretations. To avoid grain-size related trends in our paleointensity data, we need to ensure that the grainsize distribution is constant throughout the cores. Therefore we consider the $B_{1/2ARM}$ values for all samples (de Groot et al., 2013, 2015; Yu et al., 2003).

5. Results

5.1. Alboran

The Alboran core produces relatively constant Curie diagrams (Fig. 4a–c, Fig. S4) for all samples measured. The magnetization at room temperature is typically about $\sim$0.03 Am^2/kg, with Curie temperatures generally around 580 °C. One of the samples shows additional, minor peaks in magnetization around 400–500 °C, (Fig. 4b), typically explained as a contribution of pyrite. The high-field behavior of the sediments (Hcr/Hc and Mr/Ms ratios) was characterized with a Vibrating Sample Magnetometer (VSM). All samples plot in the PSD domain of the Day plot (Fig. S1). FORC diagrams reveal central ridges and no signs of diagenetic greigite (Roberts et al., 2011) (Fig. S2). Water content measurements are constant for all samples measured (Fig. S3). The magnetic susceptibility of the samples is stable (Fig. 5a) with an average bulk susceptibility of $\sim 1.5 \times 10^{-6}$ m^3/kg, implying a constant sedimentation environment. The kARM/k ratio (Fig. 5e) is also constant, except for the same 5 samples at the top of the core that deviate from the general susceptibility trend. The MAD angles associated with the interpreted directions are $<5°$ for all samples interpreted. This, in combination with the aforementioned (absent) trends in rock-magnetic parameters established the Alboran core as a reliable paleomagnetic recorder with little to no influence from environmental and/or climatic variations.

The declination varies $\pm$20–30° around its mean for the core parts (Fig. 5b). The mean inclination is around 51° and varies between 35° and 63° (Fig. 5c); these directional variations are within

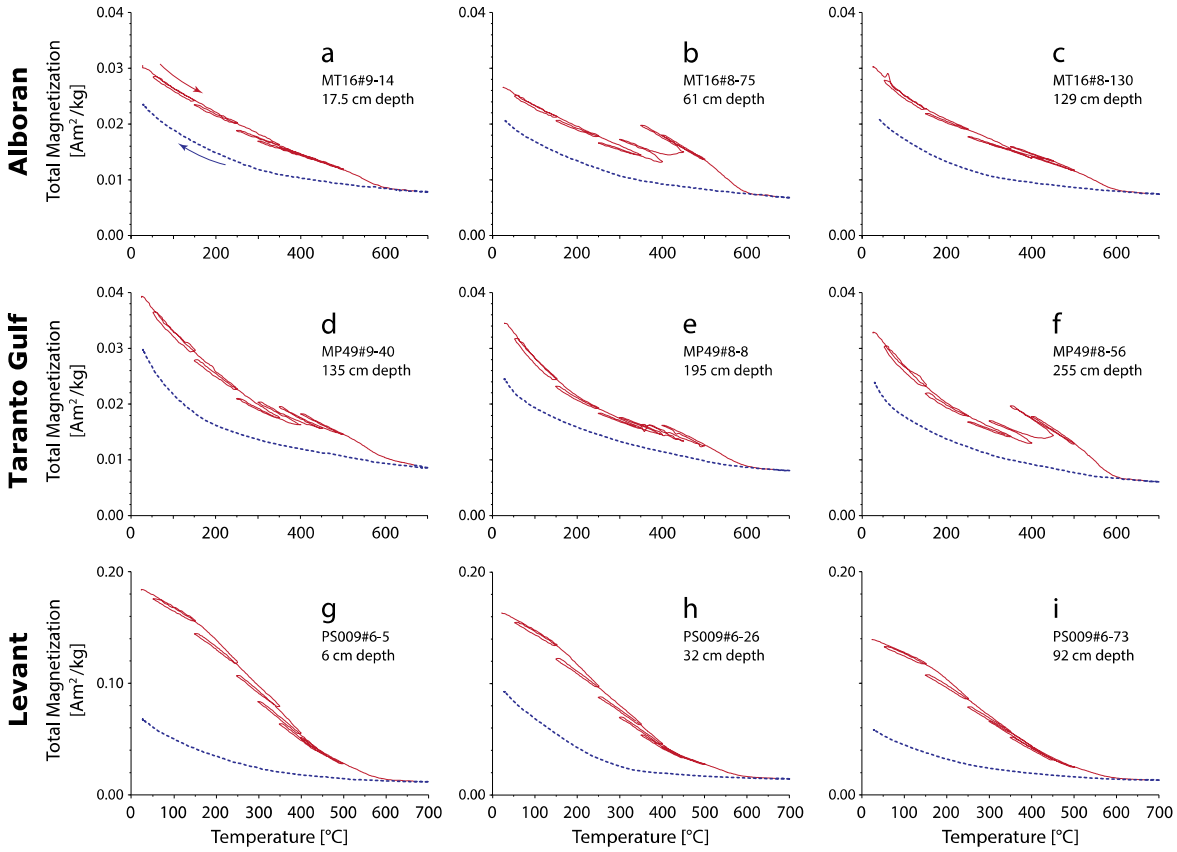

Fig. 4. Three representative thermomagnetic runs for the Alboran (a–c), Taranto Gulf (d–f) and Levant (g–i) region. Heating (red lines) and cooling (blue dashed lines) cycles are plotted as function of total magnetization. Sample code and depth within the core is indicated per sample.

the range expected for normal secular variation. The observed trends are coherent over the entire core, changes in inclination are gradual, with highest inclinations of 60–73° around depths of 50 and 130 cm. The inclination is notably low (∼35°) around 110 cm depth.

The upper part of the core reveals an episode of high intensities (Fig. 5f), between 10 and 40 cm depth, with relative paleointensities of 0.2, compared to notably lower (∼0.10–0.15) relative paleointensities in the rest of the core. There are two distinct peaks at 17 and 32 cm depth, yielding values of 0.203 and 0.199, respectively. Between 40 and 70 cm the relative paleointensity is constant at approximately 0.16, and gradually reduces to 0.12 between 70 and 110 cm depth. Notably, the $B_{1/2ARM}$, is constant throughout the core (Fig. 5f) and there are no relations between the paleointensity proxy and the grain size proxies $B_{1/2ARM}$ and kARM/k (Fig. S8), implying that the obtained paleointensity record is independent of variations in grain size of the magnetic material.

5.2. Taranto Gulf

The Curie diagrams for the Taranto Gulf core (Fig. 4d–f, Fig. S5) show room temperature magnetizations around 0.03–0.04 Am^2/kg, between 400–500 °C small additional peaks are measured. The magnetic carriers plot in the PSD part of the Day plot (Fig. S1) and FORC diagrams (Fig. S2) reveal central ridges – i.e. biogenetic greigite. The water content measurements are constant through the core (Fig. S3).

The average bulk susceptibility in the central Mediterranean core is also $\sim 1.5 \times 10^{-6}$ m^3/kg, although its magnetic susceptibility record has more variations (Fig. 5g). The upper part of this core shows a smooth variation with a small and gradual increase (∼20%) with depth, $\sim 1.8 \times 10^{-6}$ m^3/kg around a depth of 120 cm. More scattered and higher susceptibilities were measured for the lower part of the core; the magnetic susceptibility peaks at $\sim 3.3 \times 10^{-6}$ m^3/kg at a depth of 245 cm. This wide peak in susceptibility starts at a depth of 235 cm and susceptibility returns to its long-term average of $\sim 1.5 \times 10^{-6}$ m^3/kg at a depth of 260 cm. This peak also influences the kARM/k ratio (Fig. 5k), as this ratio drops for these levels, and seems to slightly increase the MAD associated with the interpreted directions (Fig. 5j). Apart from this peak, however, the Taranto Gulf core proves to be a reliable recorder of geomagnetic field variations.

The changes in declination and inclination are gradual and coherent for the Taranto Gulf core (Fig. 5h–i), even through the peak in susceptibility between 235 and 260 cm. Only the deeper part of the core (section 8) shows large variations in declination (up to ±35°); the variations in the upper part (section 9) are within ±20°. The scatter in the inclination record of the Taranto Gulf core is larger than the scatter in the Alboran core. Nevertheless, the inclination record shows a trend with depth with peaks of 70° and 75° at 120 and 200 cm, and lows of 35° at 150 and 50° at 260 cm.

The intensity (Fig. 5l) for the upper section, #9, increases with depth starting from low (0.06) intensities in the top part of the core and higher intensities (0.14) at a depth of 180 cm. The deeper section, #8, reveals maximums in intensity at depths of 190 cm and 250 cm with slopes of ∼0.11; lower intensities are present at depths of 185 cm (slope of 0.09) and 285 cm (slope decreases from 0.1 to 0.065). Although the pseudo-Thellier slope might seem to inversely correlate with the $B_{1/2ARM}$ value at first sight (Fig. 5l), no relation between these to proxies is indicated when plotted against each other (Fig. S8), or when comparing the pseudo-Thellier slope with variations in kARM/k. We therefore deem the paleointensity record reliable and independent of environmental and/or climatic variations.

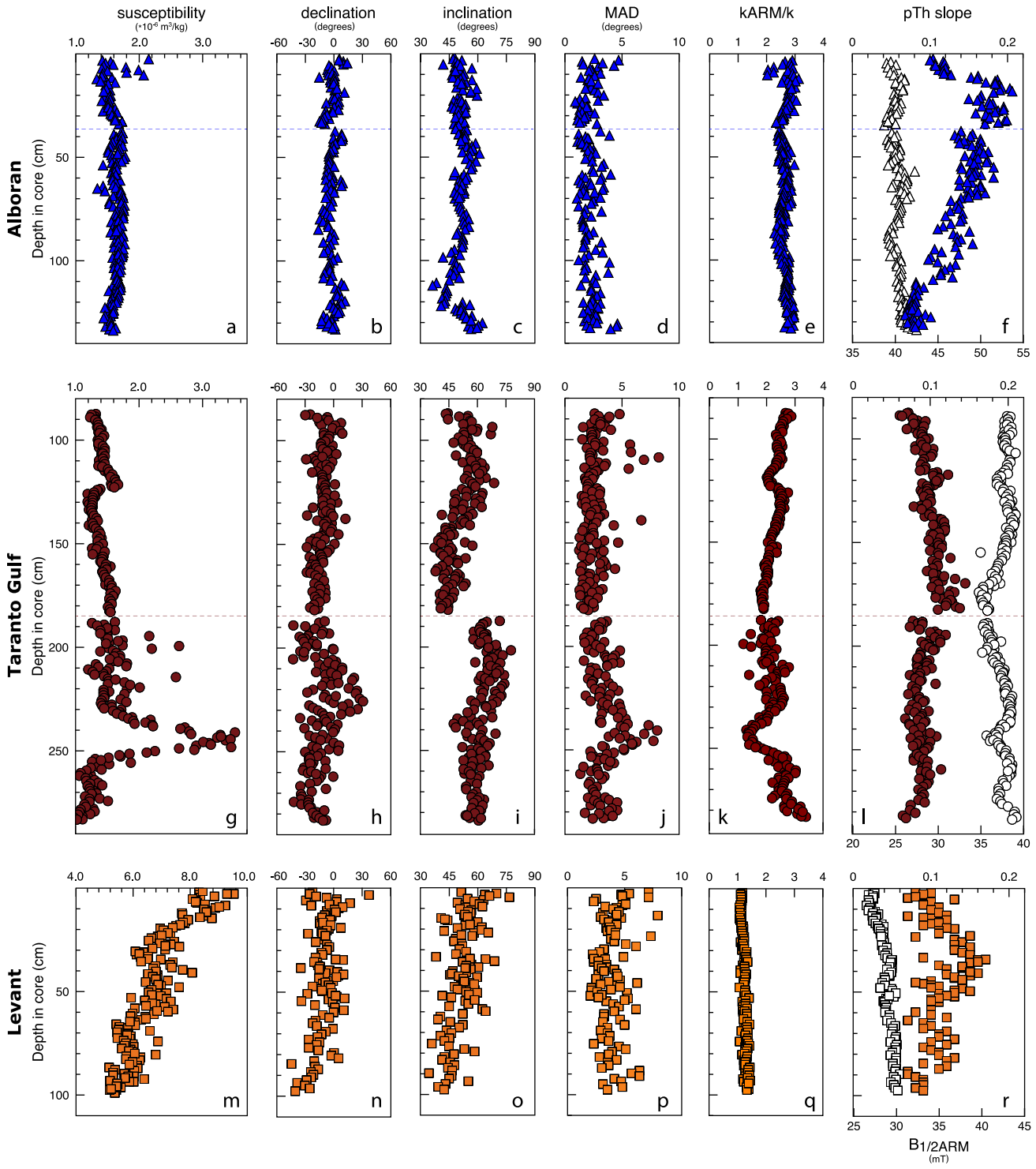

Fig. 5. Results of magnetic susceptibility, (relative) declination, inclination, mean angular deviation (MAD), kARM/k ratio, $B_{1/2ARM}$ (open symbols in panels f, l and r) and relative pseudo-Thellier (pTh) slope for all samples within the Alboran (blue triangles), Taranto Gulf (red circles) and Levant (orange squares) cores. Core sections are indicated by the dashed lines. The peak in susceptibility at a depth of 245 cm for the Taranto Gulf core is explained by an influx of volcanic material.

5.3. Levant

Samples from the Levantine core have a room temperature magnetization in the order of 0.1–0.2 Am^2/kg (Fig. 4g–i, Fig. S6), which is almost an order of magnitude higher than the other two cores. The concentration of magnetic particles in the sediment must therefore be much higher in this core compared to both the Alboran and Taranto Gulf cores. Typical Curie temperatures of 580 °C indicate magnetite as main magnetic carrier. The temperature segments between room temperature and 400 °C are not fully reversible, which may indicate the presence of greigite. FORC diagrams show central ridges indicating biogenic greigite (Fig. S2). The high-field behavior of the sediments (Hcr/Hc and Mr/Ms ratios) result in the PSD domain of the Day plot (Fig. S1); the data exhibits a minor trend: shallow samples have higher Hcr/Hc and lower Mr/Ms ratios than samples deeper within the core. This implies a small change in the grain size of remanence carrying grains,

from larger grains at the top of the core and smaller grains in the deeper parts of the core.

The Levant core, yields a scattered susceptibility record (Fig. 5m) with very high values compared to the other two cores; the average magnetic susceptibility is 7×10^{-6} m^3/kg compared to maximum susceptibilities of 3.5×10^{-6} m^3/kg for the other two cores. The susceptibility in the Levant core starts high and in the first 30 cm the signal decreases by ∼30%. Between 30 and 60 cm depth, the magnetic susceptibility increases to approximately 7.0×10^{-6} m^3/kg. For deeper parts of this core, the magnetic signal is lowest, decreasing from 6 to 5.2×10^{-6} m^3/kg. These variations may indicate changes in the sedimentary regime. The kARM/k ratio (Fig. 5q), however, is very constant at ∼1, and the $B_{1/2ARM}$ proxy (Fig. 5r) only slowly increases with depth from 26 to 30 mT. The characteristics of the magnetic minerals therefore are very constant, and the increase in susceptibility can be explained by an increase in the amount of magnetic material only; this does not influence the reliability of the paleomagnetic record.

The paleomagnetic directions in the Levant core show less coherent behavior (Fig. 5n–o), although it must be noted that the sedimentation rate in this core is lower, hence more time is averaged in each sample and high-fidelity changes are therefore less well constrained in the Levant core than in the two other cores. The overall declination and inclination vary throughout the core, with variations of ±20° for inclination and ±30° for declination. The declination shows maximums (10°–15°) at depths of 5, 32 and 82 cm, and lower values (∼−30°) at depths of 3 and 100 cm. The overall trend in declination is a decrease with depth in this core. The inclination record varies with a maximum inclination of ∼70° at a depth of ∼5 cm, minimum values (∼45°) are found at depths of 15 and 75 cm.

The intensity variations with depth for the Levant core are more scattered (Fig. 5r). The relative paleointensity is highest at a depth of 35 cm (slope of 0.13); this is approximately two times as high as the median paleointensity. Lowest intensity values (slope of 0.03) are measured at the top of the core and at 58 cm and 100 cm depths. Again, the pseudo-Thellier slope does not correlate with either the $B_{1/2ARM}$ or kARM/k grain size proxies (Fig. S8).

6. Discussion

6.1. Age models and compaction

The construction of age models for the Alboran and Taranto Gulf cores are based on three ^{14}C radiocarbon ages for each core in addition to ^{210}Pb demo measurements and show nearly linear relation with depth. Their sedimentation rates differ: a sample of 1 cm^3 contains ∼48 yr in the Alboran core and only ∼14 yr in the Taranto Gulf core. In addition, the Taranto Gulf core has a constant water content – i.e. porosity – for the sampled interval; hence compaction and thus potential inclination shallowing did not occur in this core. For the Alboran core the top most 40 cm of the core deviate from the constant water content, therefore, inclination shallowing in the top samples is possible. Deeper samples within the core are more prone to inclination shallowing, although the deeper samples for the Alboran core do not show these effects. If there is an effect of inclination shallowing for this core, it must be very small. As indicated by the ^{210}Pb analyses the top of the Alboran core was not recovered, hence the age model does not intersect the origin (Fig. 3a). The age model for samples younger than the youngest age constraint at 1675 BC (Table 2) are extrapolated from the available datings while omitting the origin and therefore less certain. The age model for the Levant core, however, is non-linear; the amount of time captured in one sample differs between the top and the bottom. The top samples cover ∼27 yr whereas the bottom samples cover approximately ∼52 yr (Hennekam et al., 2014; Hennekam and de Lange, 2012). The non-linearity of the age model can either be explained by a change in mass accumulation and/or sedimentation rate (Hennekam et al., 2014; Hennekam and de Lange, 2012), or by compaction of the sediment column through time. The water content of the sediment with depth discriminates between these two options: compaction would significantly reduce the amount of water in the sediment, while a change in sedimentation rate yields a constant water content with depth. Since the water content is constant with depth (Fig. S3), the sedimentation rate must have changed through time resulting in the non-linear age model. Compaction and the associated inclination shallowing are therefore not significant for the Levant core, nor for the other two cores.

6.2. Magnetic carriers

To obtain reliable paleomagnetic information from our cores it is important to assess the main magnetic carrier and potential variations in sedimentation regime. The main magnetic carrier for all three cores is magnetite, with a Curie temperature of 580 °C (Fig. S4–6). A small contribution of pyrite and/or greigite is present in samples from all three cores, as indicated by the thermomagnetic analyses. Pyrite is paramagnetic at room temperature and does therefore not contribute to the remanent magnetizations as measured during AF demagnetization experiments. Diagenetic greigite is known to hamper AF demagnetization experiments by the introduction of GRMs and to introduce secondary magnetizations because of later formation; while greigite of biogenic origin does not suffer from these adverse processes (Roberts et al., 2011). It is therefore paramount to characterize the nature of the greigite in our samples. FORC diagrams are capable to discriminate between diagenetic and biogenic greigite, as the latter shows up as a central ridge, and diagenetic greigite is expressed as a circular feature around 50 mT (Roberts et al., 2011). In all our FORC measurements from the three cores, the central ridge caused by biogenic greigite is evident and no signs of diagenetic greigite are present. Hence the (traces of) greigite in our samples are not expected to induce GRMs as a result of AF demagnetization experiments, and its magnetic signal is primary. This interpretation is corroborated by the lack of GRMs in our AF demagnetization experiments; all samples demagnetize towards the origin in the Zijderveld diagrams, up to 100 mT (Fig. S7).

6.3. In-core variability

Rapid variations in either one of the assessed rock magnetic proxies with depth indicate (sharp) changes in rock-magnetic behavior and hence a change in the sedimentation regime. Especially the paleointensity/VADM record is comparative in nature; it is therefore important to have constant, or only slowly changing, rock-magnetic parameters throughout our cores. These cores are marine, and for the relatively short time spans captured in these cores the nature of the sediment input is unlikely to change. Furthermore, the Taranto Gulf and Alboran cores exhibit linear sedimentation rates, whilst the sedimentation rate in the Levant core only changed gradually with depth. These relatively constant conditions are illustrated by the magnetic susceptibility records (susceptibility, Fig. 5a, g, m, and kARM/k ratios, Fig. 5e, k, q): the Alboran core has a constant susceptibility for all samples; the Taranto Gulf core shows somewhat more variability, and a peak occurring around 245 cm. This peak implies a higher concentration of magnetic material in the sediment and can be explained by the proximity to the Etna, Ischia, and Vesuvius volcanos: a higher influx of volcanic material leads to an increase in susceptibility. The susceptibility of the Levant core, however, shows a trend from higher susceptibilities in the top of the core, to lower

values at the bottom, and its susceptibility is roughly four times higher compared to the Taranto Gulf and Alboran cores. This corroborates our argument against the occurrence of compaction in this core, as compaction would increase the amount of magnetic material – hence the magnetic susceptibility – per cubic centimeter with depth, and the opposite trend is observed. Furthermore, the magnetic susceptibility results are more scattered compared to the other two cores; this scatter may lead to more variability in the paleointensity record for this core. This implies that the sedimentation regime and/or the source region of the sediment was more variable for the Levant core than for the Taranto Gulf and Alboran cores. The kARM/k ratios and $B_{1/2ARM}$ values are constant, or only slowly changing, with depth for the Alboran and Levant core. For the Taranto Gulf core more variability is observed, this can be explained by the trend in the susceptibility record for this core. More importantly, the kARM/k ratios and the $B_{1/2ARM}$ values do not show a relation with the obtained relative intensity results (Fig. S8). Hence the limited variation in concentration, composition and grain size of the magnetic carriers have no influence on the obtained paleomagnetic results and all three cores should be stable recorders of the geomagnetic field and provide reliable (relative) curves of variations in paleodirections and paleointensities.

6.4. Conversion to absolute declinations and intensities

Our relative declination record and paleointensity data can be converted to absolute full-vector descriptions of the variations in the Earth's magnetic field by pin-pointing our records using available data from the region. To this end, we obtained paleodirections and paleointensities from the GEOMAGIA database for each core location, that our coeval with our records. The geographic constraints are set to $\pm 5^\circ$ latitude by $\pm 5^\circ$ longitude for each of the three core locations, resulting in three subareas including parts of Spain and Portugal for the Alboran core; parts of Italy, the Balkan and Greece for the Taranto Gulf core; and parts of Turkey and the Levant for the Levant core. This resulted in 23, 39, and 8 paleodirections from the GEOMAGIA database for the Alboran, Taranto Gulf and Levant area, respectively (Table S2, Fig. S9). We calibrated our relative declination record to absolute declinations by using a minimum mis-fit approach. First, we obtained a 7-point moving average through our declination curves. Second, we calculated the minimum misfit to the GEOMAGIA data by summing the absolute differences between the GEOMAGIA data and our moving average, while shifting our curve with respect to the GEOMAGIA data. We selected the solution with the lowest sum of differences between the GEOMAGIA data and our moving average (Fig. S9). The available absolute declinations for the Alboran realm are all slightly younger than our youngest samples. For the Alboran record, we therefore aligned the end of our 7-point moving average for the top of our core with the only available data from GEOMAGIA.

To calibrate our relative intensity record into absolute estimates of the strength of the paleofield, we queried the GEOMAGIA database again for the same three subareas, with the single selection criterion that the data was published after the year 2000, and are coeval with our records. This resulted in 17, 20, and 81 absolute paleointensities for the Alboran, Taranto Gulf, and Levant areas, respectively. Since we know that our sedimentary samples are unable to recover the fast changes necessary for the two high peaks that occur in the Levant during the LIAA, we removed absolute paleointensity data with ages between 1200 to 700 BC for the Levant. This reduced the amount of absolute paleointensities considered for the Levant area to 25. Again, we use a minimum-misfit approach to calibrate our pseudo-Thellier slopes to absolute paleointensity estimates using a 7-point moving average through our data, and selected the solution with the lowest sum of absolute differences between the GEOMAGIA data and our moving average (Fig. S10). A list with references to all data used can be found in Table S2.

By combining our pin-pointed, relative declination and paleointensity curves with the absolute inclination record that we obtained directly from our data, we provide full-vector records of the variability in the Earth's magnetic field for the Mediterranean Sea (Fig. 6). It is important to remember that the sedimentation rate, hence the paleomagnetic resolution of our records, differs for the three cores: the Taranto Gulf core captures ~14 yr in each sample, while a data-point in the Alboran records ~48 yr. The Levant record varies from ~27 yr per sample in the top of the core, to ~52 yr per sample at the lower end of our record. Geomagnetic features on decadal timescales, such as the two short peaks reported within the LIAA (Shaar et al., 2017), will therefore remain undetected in our records.

6.5. Paleodirectional trends

The LIAA is presumed to be a strong regional, non-dipolar feature of the Earth's magnetic field (e.g. Shaar et al., 2016, 2017), it is therefore likely that the paleodirections for this period deviate more from true North than 'normal' paleosecular variation. When assuming paleosecular variation to be within 15° around a geocentric axial dipole (GAD) field the expected declination for the Alboran, Taranto Gulf, and Levant cores is within 18.3°, 19.2°, and 17.6° of true North, respectively; the expected inclination for the Alboran, Taranto Gulf, and Levant cores is 55.5° [37.6°–68.7°], 59.1° [42.8°–70.6°], and 51.5° [31.7°–65.1°], respectively (Fig. 6a, b). The directions of from the Alboran Sea and the Levant, are almost continuously within this 15° paleosecular variation limit for the entire period from 6500 BC to AD (Fig. 7b). The paleodirections produced by the Taranto Gulf deviate more than 15° from true North for the period just before and during the LIAA, from ~1500 to 700 BC. Especially the declination record from the central Mediterranean, i.e. from the Taranto Gulf core, deviates by as much as 50° to the East around 1000 BC (Fig. 6a). The largest deviations from true North are immediately preceding the occurrence of the LIAA. During this period of deviating declinations, the inclination in the Levant, and particularly in the Taranto Gulf core is steeper and towards the upper limit of 'normal' paleosecular variation. These features are not observed in our most westerly core from the Alboran Sea. Hervé et al. (2013, 2017) found similar deviations from true North for this period in time for Northwestern European data (France and Germany) and interpreted this as a dipole tilt. Nevertheless, our observed Virtual Geomagnetic Poles (VGPs) are well within normal secular variation and global geomagnetic field models such as pfm9k.1b (Nilsson et al., 2014) do not show a distinct tilted dipole during this era.

The inclinations obtained for the Taranto Gulf and Levant cores after the LIAA are shallower than the majority of the GEOMAGIA data for the Mediterranean (gray diamonds in Fig. 6, latitude: 30–50°N, longitude: −10–50°E, age: −7000 AD to 2000 AD), while the declinations agree with the literature data. This mismatch of up to 20° is currently unexplained, although the region for which the GEOMAGIA data is acquired is quite large. The directional data arises mainly from France, Greece and Bulgaria, and inclination records from the eastern and western Mediterranean are particularly scarce. In this period of rapid changes in the geomagnetic field, local variations may explain (part of) this observation.

6.6. Trends in paleointensity

The obtained absolute intensity records (Fig. 6c), result in coherent trends over time. Between 1700 and 800 BC, the trends in the Alboran (westernmost) and Taranto Gulf (central) cores agree very well, while the trends in the Taranto Gulf (central) and

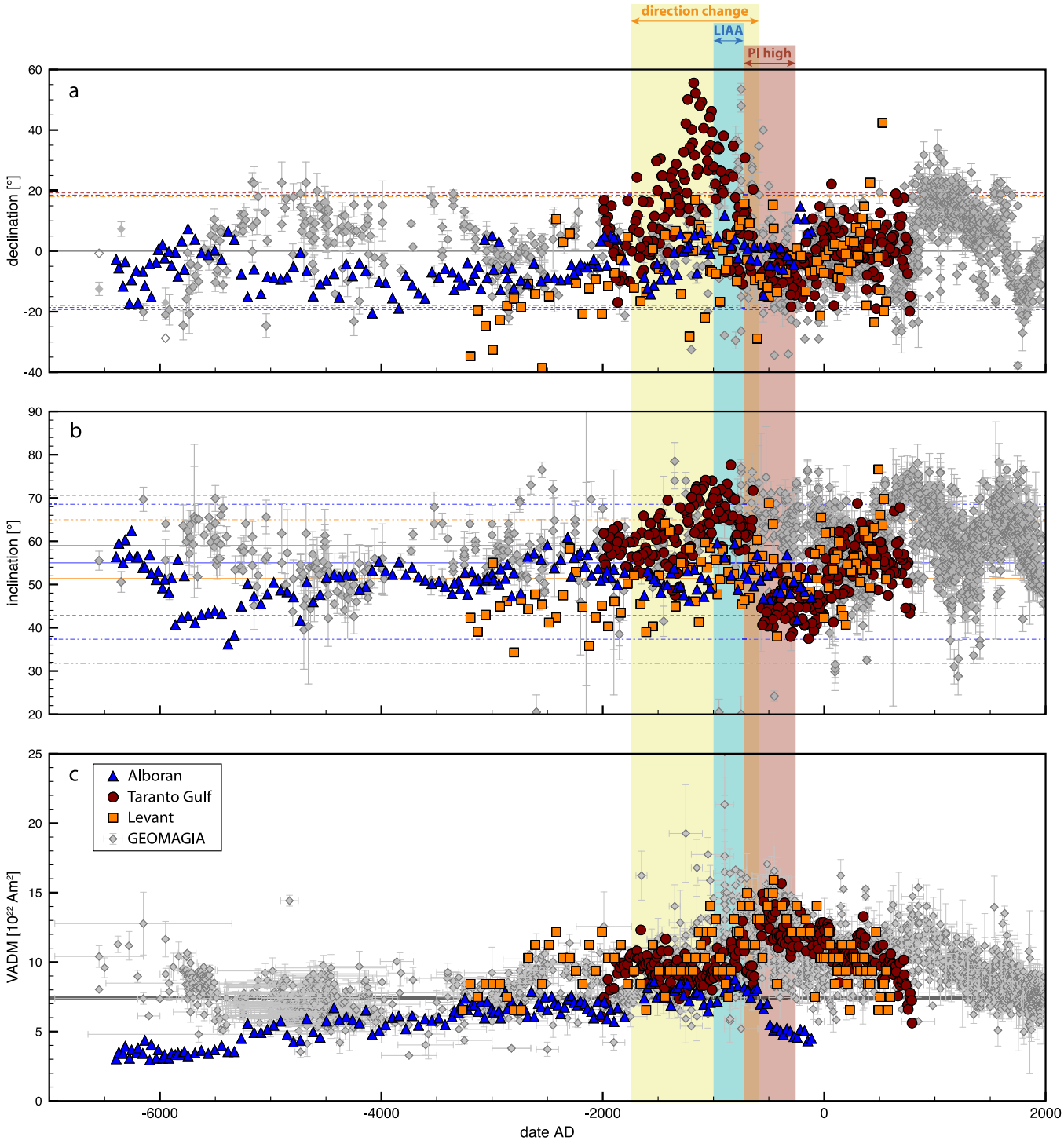

Fig. 6. Calibrated declination (a), inclination (b) and calibrated virtual axial dipole moment (VADM) (c) for the Alboran (blue triangles), Taranto Gulf (red dots) and Levant (orange squares) samples. Data from the Mediterranean region (latitude: 30–50°N, longitude: −10–50°E) available from GEOMAGIA (age interval 7000 BC to 2000 AD) is given by the grey diamonds with corresponding error bars. Expected directional (error) values for a GAD field are indicated by the colored (dashed) lines in panel a and b; the grey line (c), at $7.4 * 10^{22}$ Am^2 is the average dipole moment for the past 7 kyr (Constable, 2005). Three distinct periods are indicated in the figure, the period of directional change (yellow band) followed by a period of high paleointensities observed within our samples (red band), the period of high paleointensities observed in the LIAA is indicated by the blue band.

Levant (easternmost) cores agree between 600 BC until 500 AD (Fig. 7a). The paleointensities from the top 10 cm of the Alboran core (430 BC to 0 AD), however, deviate distinctly from the other two cores, and from all literature data reported so far. As these samples are from the top of the core they are more likely to be affected by post-recovery processes – i.e. chemical alteration due to oxidation, that affects the pseudo-Thellier results obtained from these samples, although there are no signs of this in the rock-magnetic proxies and we have no empirical or theoretical reason to disregard this data. The age-model for the top of the Alboran core, however, is not very well defined. The ages after 1675 BC are an extrapolation of the datings that are available (Table 2), while the top of the sediment was not recovered. Even if the sedimentation rate in the Alboran core would suddenly decrease after 1675

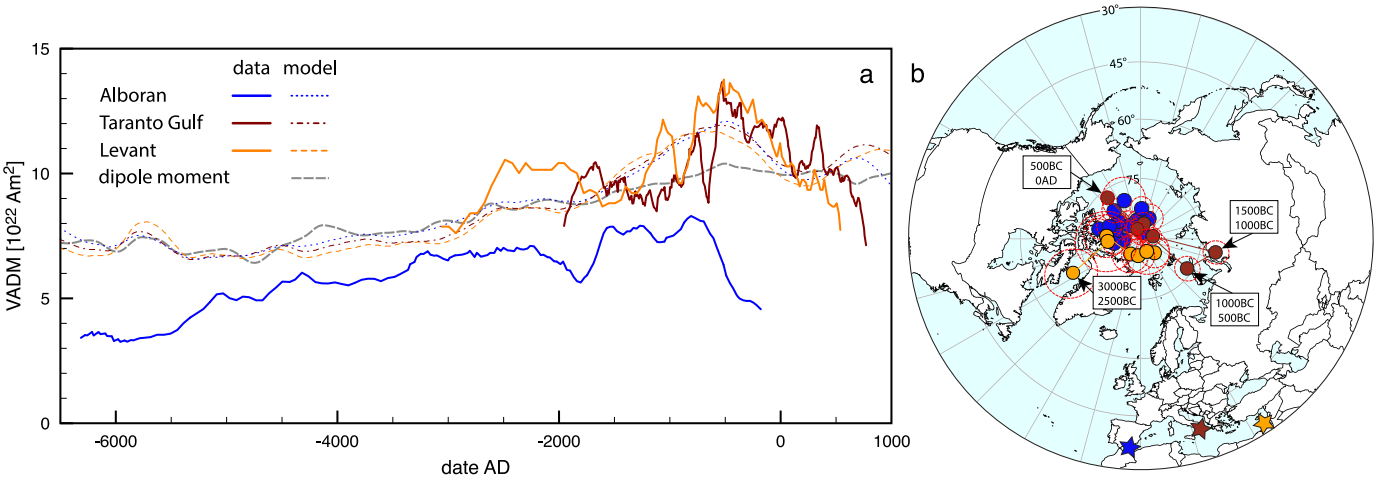

Fig. 7. Comparison of the Virtual Axial Dipole Moments (VADMs) of our three cores (a). The curves are produced using a seven-point moving average from the data in Fig. 6c (Alboran in blue, Taranto Gulf in red, and Levant in orange); the pfm9k.1b model (Nilsson et al., 2014) was evaluated for the three locations (dashed lines in corresponding color) and the dipole moment of pfm9k (grey dashed line). Paleosecular variation (PSV) curves (b) for the Alboran (blue dots), Taranto Gulf (red dots) and Levant (orange dots) samples. Virtual Geomagnetic Pole locations are given in 500 yr bins with alpha95 confidence cones (red dotted circles).

BC and the sudden decrease in intensities would be smoothed in time, this trend is not observed in the Taranto Gulf and Levant sections. This implies that the geomagnetic field strength in the Western Mediterranean dropped sharply while the intensities in the Eastern and Middle part of the Mediterranean continued to rise between 800 and 200 BC. The deeper parts of the Alboran core reveal a gradual increase of the geomagnetic field from ~35 ZAm^2 around 6000 BC, to ~80 ZAm^2 just before the occurrence of the LIAA around 1000 BC.

The Levant and Taranto Gulf data reveal a distinct period of higher intensities with their peak shortly after the occurrence of the LIAA, between 750 and 250 BC, with its maximum of ~150 ZAm^2 (Fig. 6c, smoothed to ~135 ZAm^2 in Fig. 7a) occurring at 500 BC for both locations. This agrees well with literature data obtained from the GEOMAGIA database for the entire Mediterranean region (Fig. 6c). As expected due to the nature of our samples the very short-lived spikes within the LIAA are not recovered.

6.7. The nature and evolution of the LIAA

The paleodirections of the Alboran and Taranto Gulf cores generally exhibit relatively shallow inclinations leading to VGP positions just North of Canada, but within normal paleosecular variation (Fig. 6b–c, Fig. 7b). For the Taranto Gulf core we observe steeper inclinations leading to a VGP North of Russia, during a short period of time just before the onset of the LIAA (1500–500 BC). The Levant core produces paleodirections pointing to VGPs that are more on the Eastern hemisphere, towards Russia; but also within normal paleosecular variation. The higher paleointensities in the Taranto Gulf and Levant cores between 1000 BC and 0 AD correspond to the periods of relatively steeper inclinations in these cores, although the steep inclinations seem to occur during the onset of the higher paleointensities (Fig. 6). Stronger paleointensities in combination with steeper inclinations can be tentatively explained by a stronger and tilted dipole (e.g. Hervé et al., 2017); although a presumed tilt in the dipole cannot be characterized by data from the Mediterranean realm alone. The slight miss-match between the steep inclinations and the high paleointensities in time, the absence of steep inclinations in the Alboran core, and relatively low paleointensities in the Alboran core emphasize the regional character of the LIAA. This, in combination with a lack of dipole tilt in global geomagnetic models such as pfm9k.1b (Nilsson et al., 2014), illustrates that the behavior of the Earth's magnetic field was largely non-dipolar during the period of high paleointensities in the Levant and Mediterranean area in the first millennium BC. This is confirmed by comparing the VADMs of our three locations with the dipole moment of the pfm9k.1b-model (Fig. 7a). Especially between 1000 BC and 0 AD, our data, as well as the pfm9k.1b-model evaluated for our three locations, deviate sharply from the dipole moment of this model.

Recently, Shaar et al. (2017) discussed the quality of intensity data obtained from GEOMAGIA for five different areas near the Levant from 5000 BC to 2000 AD. Our continuous full-vector records for the Mediterranean expand our knowledge on the behavior of the LIAA westwards and therefore broaden the regional analyses presented in Shaar et al. (2017). When combining the high-quality data as discussed by Shaar et al. (2017) with high-quality data from the Canary Islands (de Groot et al., 2015; Kissel et al., 2015), and our newly produced intensity records for the Mediterranean we can map the geomagnetic field intensity over time; starting at 1000 BC with time intervals of 250 yr to 250 AD (Fig. 8). The highest paleointensities (VADMs > 140 ZAm^2) are observed between 1000 and 500 BC for regions East of the Levant, and the Levant itself. From 500 BC onwards the intensity of the peak decays, while the location of the highest paleointensities moves slightly westwards.

The low paleointensities obtained from the Alboran core taken South of Spain provide a hard, western limit of the extent of the LIAA, at least until 250 BC. The relatively high paleointensities observed for the Canary Islands between 1000 and 500 AD are therefore geographically disconnected from the LIAA by the much lower paleointensities from our Alboran site. Since the intensities for the Canary Islands are relatively high already from 1000 BC onwards independently of the occurrence of the LIAA, it seems unlikely that the high intensities for that location around AD would be directly linked to the westward movement of the LIAA. Therefore, we disregard the Canary Island data while assessing this westward movement. The LIAA moves from 40 to 55° East at 1000 BC to ~25° East at AD, while decaying from ~150 ZAm^2 to ~110 ZAm^2 in the same time span. This results in a westward movement of 15–30° in 1000 yr.

7. Conclusion

Based on three well-dated marine sediment cores taken from the West (Alboran Sea), Central (Taranto Gulf), and East Mediterranean (Levantine basin), we provide continuous full-vector records of the variations in the geomagnetic field for this region dur-

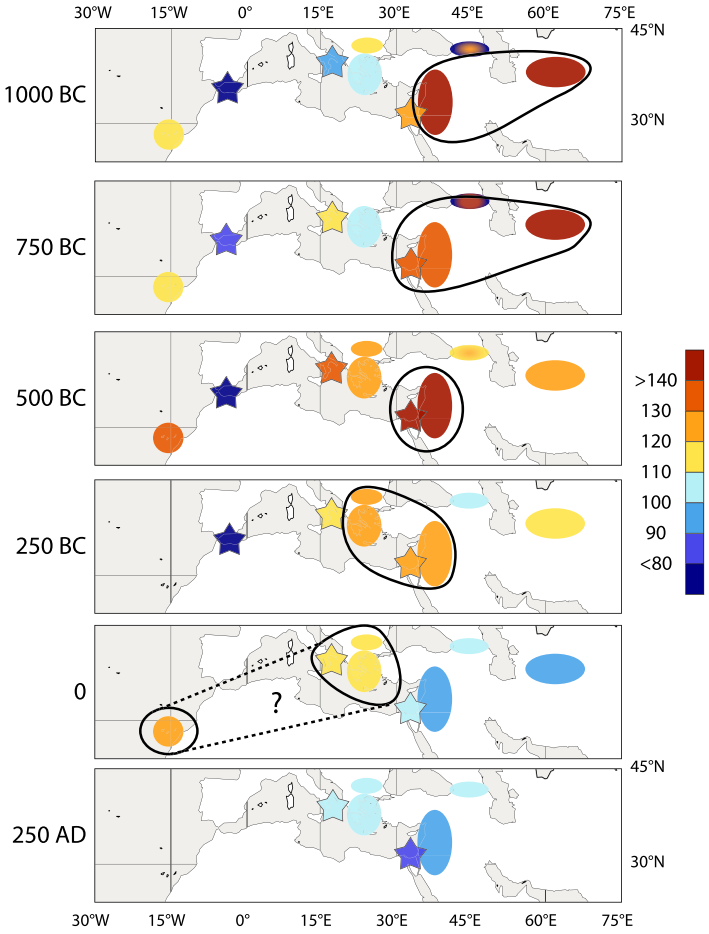

Fig. 8. Geomagnetic field intensity over time. Locations of the sediment cores are indicated with a star, the circular shapes are the data areas from the Canary Island (de Groot et al., 2015; Kissel et al., 2015) and the five areas as discussed in Shaar et al. (2017); the colors represent the virtual axial dipole moment in ZAm^2 averaged for the area and corresponding time. Latitude and longitudes are displayed in the upper and lower panel by the grey values. The area for which the highest field values – for the corresponding time – are reported is given by the black circle.

ing a period of known high intensities in the Levant, the LIAA. These cores expand the regional constraints on the occurrence of the LIAA westwards. Low intensities obtained from the Alboran core South of Spain provide a hard, western limit for the LIAA at least until 250 BC. Comparing our other two records with data previously analyzed for the Levant and areas East of the Levant, we observe the LIAA to move westwards at a rate of 15–30° in 1000 yr, while decaying in field strength from ∼150 ZAm^2 to ∼110 ZAm^2 in the same time span. A connection of the LIAA with the relatively high paleointensities reported for the Canary Islands from 1000 BC onwards is unlikely due to the low paleointensities obtained from our Alboran core.

Acknowledgements

We thank an anonymous reviewer who greatly helped to improve this manuscript. LVdG acknowledges NWO VENI grant 863.15.003.

Appendix A. Supplementary material

Supplementary material related to this article can be found online at https://doi.org/10.1016/j.epsl.2019.01.021.

References

Almogi-Labin, A., Bar-Matthews, M., Shriki, D., Kolosovsky, E., Paterne, M., Schilman, B., Ayalon, A., Aizenshtat, Z., Matthews, A., 2009. Climatic variability during the last ∼90 ka of the southern and northern Levantine Basin as evident from marine records and speleothems. Quat. Sci. Rev. 28, 2882–2896. https://doi.org/10.1016/j.quascirev.2009.07.017.

Banerjee, S.K., King, J., Marvin, J., 1981. A rapid method for magnetic granulometry with applications to environmental studies. Geophys. Res. Lett. 8 (4), 333–336. https://doi.org/10.1029/GL008i004p00333.

Ben-Yosef, E., Millman, M., Shaar, R., Tauxe, L., Lipschits, O., 2017. Six centuries of geomagnetic intensity variations recorded by royal Judean stamped jar handles. Proc. Natl. Acad. Sci. USA 114, 2160–2165. https://doi.org/10.1073/pnas.1615797114.

Ben-Yosef, E., Tauxe, L., Levy, T.E., Shaar, R., Ron, H., Najjar, M., 2009. Geomagnetic intensity spike recorded in high resolution slag deposit in Southern Jordan. Earth Planet. Sci. Lett. 287, 529–539. https://doi.org/10.1016/j.epsl.2009.09.001.

Bourne, M.D., Feinberg, J.M., Stafford Jr., T.W., Waters, M.R., Lundelius Jr., E., Forman, S.L., 2016. High-intensity geomagnetic field "spike" observed at ca. 3000 cal BP in Texas, USA. Earth Planet. Sci. Lett. 442 (C), 80–92. https://doi.org/10.1016/j.epsl.2016.02.051.

Brown, M.C., Donadini, F., Korte, M., Nilsson, A., Korhonen, K., Lodge, A., Lengyel, S.N., Constable, C.G., 2015. GEOMAGIA50.v3: 1. general structure and modifications to the archeological and volcanic database Recent advances in environmental magnetism and paleomagnetism. Earth Planets Space 67, 1333. https://doi.org/10.1186/s40623-015-0232-0.

Constable, C., 2005. Dipole moment variation. In: Encyclopedia of Geomagnetism and Paleomagnetism. Springer, Dordrecht, pp. 159–161.

Day, R., Fuller, M., Schmidt, V.A., 1977. Hysteresis properties of titanomagnetites: grain-size and compositional dependence. Phys. Earth Planet. Inter. 13, 260–267. https://doi.org/10.1016/0031-9201(77)90108-x.

Di Chiara, A., Tauxe, L., Speranza, F., 2014. Paleointensity determination from São Miguel (Azores Archipelago) over the last 3 ka. Phys. Earth Planet. Inter. 234 (C), 1–13. https://doi.org/10.1016/j.pepi.2014.06.008.

Dunlop, D.J., 2002. Theory and application of the Day plot (M_{rs}/M_s versus H_{cr}/H_c), 1: theoretical curves and tests using titanomagnetite data. J. Geophys. Res. 107 (B3), 7069-22. https://doi.org/10.1029/2001JB000486.

de Groot, L.V., Beguin, A., Kosters, M.E., van Rijsingen, E.M., Struijk, E.L.M., Biggin, A.J., Hurst, E.A., Langereis, C.G., Dekkers, M.J., 2015. High paleointensities for the Canary Islands constrain the Levant geomagnetic high. Earth Planet. Sci. Lett. 419, 154–167. https://doi.org/10.1016/j.epsl.2015.03.020.

de Groot, L.V., Biggin, A.J., Dekkers, M.J., Langereis, C.G., Herrero-Bervera, E., 2013. Rapid regional perturbations to the recent global geomagnetic decay revealed by a new Hawaiian record. Nat. Commun. 4, 1–7. https://doi.org/10.1038/ncomms3727.

Goudeau, M.-L.S., Reichart, G.J., Wit, J.C., de Nooijer, L.J., Grauel, A.L., Bernasconi, S.M., de Lange, G.J., 2015. Seasonality variations in the Central Mediterranean during climate change events in the Late Holocene. Palaeogeogr. Palaeoclimatol. Palaeoecol. 418, 304–318. https://doi.org/10.1016/j.palaeo.2014.11.004.

Harrison, R.J., Feinberg, J.M., 2008. FORCinel: an improved algorithm for calculating first-order reversal curve distributions using locally weighted regression smoothing. Geochem. Geophys. Geosyst. 9 (5). https://doi.org/10.1029/2008GC001987.

Hennekam, R., de Lange, G., 2012. X-ray fluorescence core scanning of wet marine sediments: methods to improve quality and reproducibility of high-resolution paleoenvironmental records. Limnol. Oceanogr., Methods 10, 991–1003. https://doi.org/10.4319/lom.2012.10.991.

Hennekam, R., Jilbert, T., Schnetger, B., De Lange, G.J., 2014. Solar forcing of Nile discharge and sapropel S1 formation in the early to middle Holocene eastern Mediterranean. Paleoceanography 29, 343–356. https://doi.org/10.1002/2013PA002553.

Hervé, G.L., Faßbinder, J., Gilder, S.A., Metzner-Nebelsick, C., Gallet, Y., Genevey, A., et al., 2017. Fast geomagnetic field intensity variations between 1400 and 400 BCE: new archaeointensity data from Germany. Phys. Earth Planet. Inter. 270, 143–156. https://doi.org/10.1016/j.pepi.2017.07.002.

Hervé, G.L., Chauvin, A., Lanos, P., 2013. Geomagnetic field variations in Western Europe from 1500 BC to 200 AD, part II: new intensity secular variation curve. Phys. Earth Planet. Inter. 218 (C), 51–65. https://doi.org/10.1016/j.pepi.2013.02.003.

Hughen, K., Lehman, S., Southon, J., Overpeck, J., Marchal, O., Herring, C., Turnbull, J., 2004. ^{14}C activity and global carbon cycle changes over the past 50,000 years. Science 303, 202–207. https://doi.org/10.1126/science.1090300.

King, J., Banerjee, S.K., Marvin, J., Özdemir, Ö., 1982. A comparison of different magnetic methods for determining the relative grain size of magnetite in natural materials: some results from lake sediments. Earth Planet. Sci. Lett. 59 (2), 404–419. https://doi.org/10.1016/0012-821X(82)90142-X.

Kissel, C., Laj, C., Rodriguez-Gonzalez, A., Perez-Torrado, F., Carracedo, J.C., Wandres, C., 2015. Holocene geomagnetic field intensity variations: contribution from the low latitude Canary Islands site. Earth Planet. Sci. Lett. 430 (C), 178–190. https://doi.org/10.1016/j.epsl.2015.08.005.

Koymans, M.R., Langereis, C.G., Pastor-Galán, D., van Hinsbergen, D.J.J., 2016. Paleomagnetism.org_An online multi-platform open source environment for paleomagnetic data analysis. Comput. Geosci. 93, 127–137. https://doi.org/10.1016/j.cageo.2016.05.007.

Liu, Q., Roberts, A.P., Larrasoaña, J.C., Banerjee, S.K., Guyodo, Y., Tauxe, L., Oldfield, F., 2012. Environmental magnetism: principles and applications. Rev. Geophys. 50 (4), Q05Z24-50. https://doi.org/10.1029/2012RG000393.

Mullender, T.A.T., van Velzen, A.J., Dekkers, M.J., 1993. Continuous drift correction and separate identification of ferrimagnetic and paramagnetic contributions in thermomagnetic runs. Geophys. J. Int. 114, 663–672. https://doi.org/10.1111/j.1365-246X.1993.tb06995.x.

Mullender, T.A.T., Frederichs, T., Hilgenfeldt, C., de Groot, L.V., Fabian, K., Dekkers, M.J., 2016. Automated paleomagnetic and rock magnetic data acquisition with an in-line horizontal "2G" system. Geochem. Geophys. Geosyst. 17, 3546–3559. https://doi.org/10.1002/2016GC006436.

Nilsson, A., Holme, R., Korte, M., Suttie, N., Hill, M., 2014. Reconstructing Holocene geomagnetic field variation: new methods, models and implications. Geophys. J. Int. 198 (1), 229–248. https://doi.org/10.1093/gji/ggu120.

Roberts, A.P., Chang, L., Rowan, C.J., Horng, C.-S., Florindo, F., 2011. Magnetic properties of sedimentary greigite (Fe_3S_4): an update. Rev. Geophys. 49, 1233–1246. https://doi.org/10.1029/2010RG000336.

Shaar, R., Ben-Yosef, E., Ron, H., Tauxe, L., Agnon, A., Kessel, R., 2011. Geomagnetic field intensity: how high can it get? How fast can it change? Constraints from Iron Age copper slag. Earth Planet. Sci. Lett. 301, 297–306. https://doi.org/10.1016/j.epsl.2010.11.013.

Shaar, R., Tauxe, L., Goguitchaichvili, A., Devidze, M., Licheli, V., 2017. Further evidence of the Levantine Iron Age geomagnetic anomaly from Georgian pottery. Geophys. Res. Lett. 26, 3–8. https://doi.org/10.1002/2016GL071494.

Shaar, R., Tauxe, L., Ron, H., Ebert, Y., Zuckerman, S., Finkelstein, I., Agnon, A., 2016. Large geomagnetic field anomalies revealed in Bronze to Iron Age archeomagnetic data from Tel Megiddo and Tel Hazor, Israel. Earth Planet. Sci. Lett. 442, 173–185. https://doi.org/10.1016/j.epsl.2016.02.038.

Siani, G., Paterne, M., Arnold, M., Bard, E., Métivier, B., Tisnerat, N., Bassinot, F., 2000. Radiocarbon reservoir ages in the Mediterranean Sea and Black Sea. Radiocarbon 42, 271–280. https://doi.org/10.1017/S0033822200059075.

Stuiver, M., Reimer, P.J., 1993. Extended ^{14}C data base and revised CALIB 3.0 ^{14}C age calibration program. Radiocarbon 35, 215–230. https://doi.org/10.1017/S0033822200013904.

Stuiver, M., Reimer, P.J., Braziunas, T.F., 1998. High-precision radiocarbon age calibration for terrestrial and marine samples. Radiocarbon 40, 1127–1151. https://doi.org/10.1017/S0033822200019172.

Tauxe, L., Pick, T., Kok, Y.S., 1995. Relative paleointensity in sediments: a pseudo-Thellier approach. Geophys. Res. Lett. 22, 2885–2888. https://doi.org/10.1029/95GL03166.

Vasiliev, I., Franke, C., Meeldijk, J.D., Dekkers, M.J., Langereis, C.G., Krijgsman, W., 2008. Putative greigite magnetofossils from the Pliocene epoch. Nat. Geosci. 1, 782–786. https://doi.org/10.1038/ngeo335.

Venkatarathnam, K., Ryan, W.B.F., 1971. Dispersal patterns of clay minerals in the sediments of the eastern Mediterranean Sea. Mar. Geol. 11, 261–282. https://doi.org/10.1016/0025-3227(71)90028-4.

Yu, Y., Dunlop, D.J., Özdemir, Ö., 2003. Are ARM and TRM analogs? Thellier analysis of ARM and pseudo-Thellier analysis of TRM. Earth Planet. Sci. Lett. 205, 325–336. https://doi.org/10.1016/S0012-821X(02)01060-9.